

Diffraction grating couplers milled in Si₃N₄ rib waveguides with a focused ion beam

Kirill E. Zinoviev, Carlos Dominguez

*Instituto de Microelectronica de Barcelona CNM CSIC, Campus UAB,
08193, Cerdanyola, Barcelona, Spain
kirill.zinoviev@cnm.es*

Anna Vilà

*EME/CeRMAE/CEMIC. Electronics department, University of Barcelona, Martí i Franqués 1,
E-08028-Barcelona, Spain*

Abstract: Focused ion beam milling is a processing technology which allows flexible direct writing of nanometer scale features efficiently substituting electron beam lithography. No mask need results in ability for patterns writing even on fragile micromechanical devices. In this work we studied the abilities of the tool for fabrication of diffraction grating couplers in silicon nitride waveguides. The gratings were fabricated on a chip with extra fragile cantilevers of sub micron thickness. Optical characterization of the couplers was done using excitation of the waveguides in visible range by focused Gaussian beams of different waist sizes. Influence of Ga⁺ implantation on the device performance was studied.

©2005 Optical Society of America

OCIS codes: (050.1950) diffraction gratings; (220.4000) microstructure fabrication; (130.2790) guided waves.

References and links

1. D. Wiesmann, C. David, R. Germann, D. Erni, and G. L. Bona, "Apodized Surface-Corrugated Gratings With Varying Duty Cycles," *IEEE Photon. Technol. Lett.*, **12**, 639-642 (2000).
2. Andrei Y. Smuk and Nabil M. Lawandy, "Direct laser writing diffractive optics in glass," *Opt. Lett.* **22**, 1030 (1997).
3. N. Destouches, A. V. Tishchenko, J. C. Pommier, S. Reynaud, O. Parriaux, S. Tonchev, M. Abdou Ahmed, "99% efficiency measured in the -1st order of a resonant grating," *Opt. Express* **13**, 3230-3235 (2005).
<http://www.opticsexpress.org/abstract.cfm?URI=OPEX-13-9-3230>
4. Darren Freeman, and Barry Luther-Davis, "Fabrication of planar photonic crystals in chalcogenide glass using a focused ion beam," *Opt. Express* **13**, 3079-3086 (2005).
<http://www.opticsexpress.org/abstract.cfm?URI=OPEX-13-8-3079>
5. Yongqi Fu, Ngoi Kok Ann Bryan, and Wei Zhou, "Self-organized formation of Blazed-grating-like structure on Si(100) induced by focused ion beam scanning," *Opt. Express* **12**, 227-233 (2004).
<http://www.opticsexpress.org/abstract.cfm?URI=OPEX-12-2-227>
6. Yongqi Fu, Ngoi Kok Ann Bryan, and Wei Zhou, "Quasi-direct writing of diffractive structures with a focused ion beam," *Opt. Express* **12**, 1803-1809 (2004).
<http://www.opticsexpress.org/abstract.cfm?URI=OPEX-12-9-1803>
7. V. G. Ta'eed, D. J. Moss, B. J. Eggleton, D. Freeman, S. Madden, M. Samoc and B. Luther-Davies, S. Janz, D.-X. Xu, "Bragg gratings in silicon-on-insulator waveguides by focused ion beam milling," *Appl. Phys. Lett.* **85**, 4860-4862 (2004)
8. Ampere A Tseng, "Recent developments in micromilling using focused ion beam technology," *J. Micromech. Microeng.* **14**, R15-R34 (2004).
9. R.Petit, "Electromagnetic Theory of gratings," (Springer Berlag, Berlin 1980).
10. W. Streifer, R.D. Burnham, and D.R. Scifres, "Analysis of grating coupled radiation in GaAs:GaAlAs lasers and waveguides," *IEEE J. Quantum Electron.* **QE-12**, 422-428 (1976)
11. John C. Brazas, Lifeng Li, "Analysis of input grating couplers having finite lengths," *Appl. Opt.* **34**, 3786-3792 (1995)
12. Lifeng Li Mool C.Gupta, "Effects of beam focusing on the efficiency of planar grating couplers," *Appl. Opt.* **29**, 5320-5325 (1990).

13. N. Eriksson, M. Hagberg, A. Larson, "Highly Directional Grating OutCouplers with Tailorable Radiation Characteristics," *IEEE J. Quantum Electron.* **32**, 1038-1047 (1996)
14. Yongqi Fu, N.K.A. Brayan, "Investigation of physical properties of quartz after focused ion beam bombardment," *Appl. Phys. B* **80**, 581-585, (2005).

1. Introduction

Diffraction gratings with sub-micron period can be fabricated using electron beam lithography [1], laser direct writing [2], optical holography [3], or focused ion beam [4-8]. Focused ion beam (FIB) milling is a processing technology which allows flexible direct writing of nanometer scale features efficiently substituting electron beam lithography [7]. No mask need results in ability for patterns writing with well controlled profile and depth of the grooves [4]. It can be used as a post fabricated tool for patterns generation on even fragile micromechanical devices [8]. This is what currently can not be done with any other fabrication technology and this is probably the major advantage of the method.

Although the method seems to be simple, milling with FIB is a complicated process. Energetic ions hitting the target produce a variety of ion-target interactions [8]. Apart from the physical removal of the target material it can produce implantation of the ions into the target [7, 8]. Nowadays the majority of ion sources currently available are the liquid metals (Ga, Au, Cu, Cs, Fe, Al, and etc.). The presence of implanted metal in the optical waveguides introduces absorption of light and affects the performance of the fabricated devices [7]. In this work we studied the properties of diffraction grating couplers in silicon nitride waveguides designed to work in visible range and fabricated by FIB milling technology.

Diffraction grating coupler (DGC) is a frequently used element for out of plane light coupling in or out of planar waveguides of sub-micron thickness employed in integrated optics. DGC facilitates alignment and reduces the size of the optical systems compared, for example, to the ones using the end-fire or the prism coupling. Dielectric periodic waveguides have been intensively studied over the last several decades [9-13] and a solid platform for their modeling has been created. According to the theory of the dielectric periodic waveguides the most important parameter defining the properties of the couplers is the radiation loss, normalized measure of the power radiated by corrugated structure per unit length [10]. It is inverse proportional to the optimum excitation length of the coupler. This implies that the optimized excitation of the waveguide on DGC must be performed with the light beam of a certain size w (see Fig.1). Normally the waveguides with shallow gratings are excited by wide beams, while deep corrugation needs tightly focused beams [11-12].

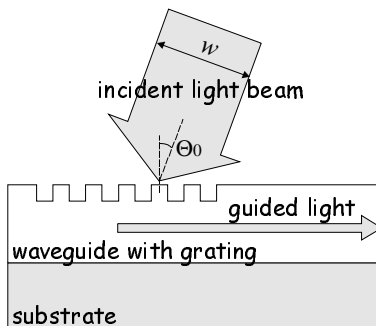


Fig. 1. Excitation of the waveguide by out of plane incident beam with diameter w

2. Gratings fabrication

The gratings were fabricated on a chip which is $3 \times 7 \text{ mm}^2$ in size and contains, apart from the waveguides, very fragile cantilevers fabricated by bulk micromachining (see Fig. 2). The gratings were designed for out of plane light coupling into waveguides. The coupling was to be realized on a rectangular grating etched in silicon nitride waveguide deposited over a

silicon substrate and isolated of it by silica layer. Coupling should be done using -1^{st} order of diffraction with a Gaussian beam of TE polarization at 632.8 nm wavelength. The grating period was set to 320 nm while the grating profile should have a rectangular shape with duty cycle of 0.5 and depth of 20 nm. The optimized coupler length should be about 36 μm .

The sample was fabricated using standard silicon technologies: Thermal silicon dioxide buffer layer of 1.5 μm thick was grown on silicon substrate. Then silicon nitride waveguide layer with refractive index 2.03 was deposited using LPCVD technique. Afterwards 40 μm wide and 140 nm thick rib waveguides were defined using standard photolithography followed by reactive ion etching. The identical waveguides had been characterized to find absorption losses, which did not exceed 0.5 cm^{-1} . The gratings were located 1 mm off the chip edge. Thus absorption as well as scattering on the imperfections of the waveguide surface was neglected in the experiments due to the short propagation length of light along the waveguides. The facets of the waveguides were made right at the edge of the chip. This was to facilitate light in-coupling into the waveguides using direct focusing on the facets and light out-coupling from the waveguides.

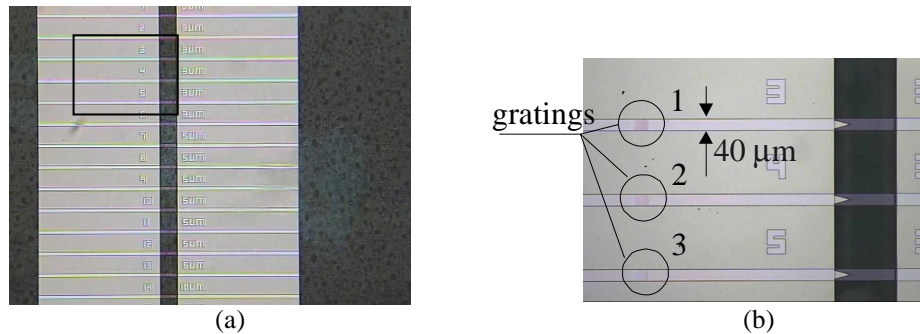


Fig. 2. (a) A photograph of a chip with waveguides and cantilevers (the waveguides in the cavities are the cantilevers of sub-micron thickness). (b) A magnified photo of the chip area with gratings (marked by the frame in fig. 2(a)). The gratings are $40 \times 40 \mu\text{m}^2$ in size

The dual-beam FEI Strata235 FIB system has been used for gratings fabrication, having both electron and ion beams for imaging and working. The FIB was mounted at an angle of 52° to the Scanning Electron Microscopy (SEM) column, and the sample can be tilted to face either beam. A Liquid Metal Source provides Ga ions which are accelerated to 30 keV and deflected electronically to focus on the same point than the electron beam, which is emitted by a Field Emission Gun and accelerated to 5 keV. Intensity of the ion beam can be varied and is continuously monitored, and for this work it was near 230 pA.

The gratings were fabricated using a single pass technique adjusting the ion beam size to the grating line width. The dwell time for the milling of groove lines was being changed in order to fabricate three gratings of different depth, which implies different ion dose was applied to each grating. Time for milling was 5 seconds per line for the first grating, 3 and 2 seconds per line for the second and for the third ones correspondingly. The data on the obtained gratings are presented in the Table 1.

Table 1. Parameters of the diffraction grating couplers

Grating	Dose, Ga ions per cm^2	Period, nm	Corrugation depth, nm	Expected propagation constant, μm^{-1}	Measured propagation constant, μm^{-1}
1	$8.9 \cdot 10^{16}$	320	20	16.59	17.04
2	$5.4 \cdot 10^{16}$	316	8	16.760	17.16
3	$3.6 \cdot 10^{16}$	310	5	16.79	17.38

The depth of the grating grooves (lines) is a function of the applied dose. The period of the gratings slightly varies from one grating to the other, what was caused by limited precision of the translation stage positioning the sample with respect to the ion beam. The data on the propagation constants of the waveguides, obtained using the setup described in the next section, is also presented in the table.

The quality of the corrugation pattern can be observed in Fig. 3, where the grating profile obtained by AFM and a spectrum of the profile are presented. It can be observed on the picture that the grooves have V-shape profile which is a consequence of the Gaussian distribution of the ions in the ion beam [8]. However, the distribution of the main spatial harmonics in the profile spectrum (see Fig. 3(b)) reminds the spectrum of the rectangular pulse train.

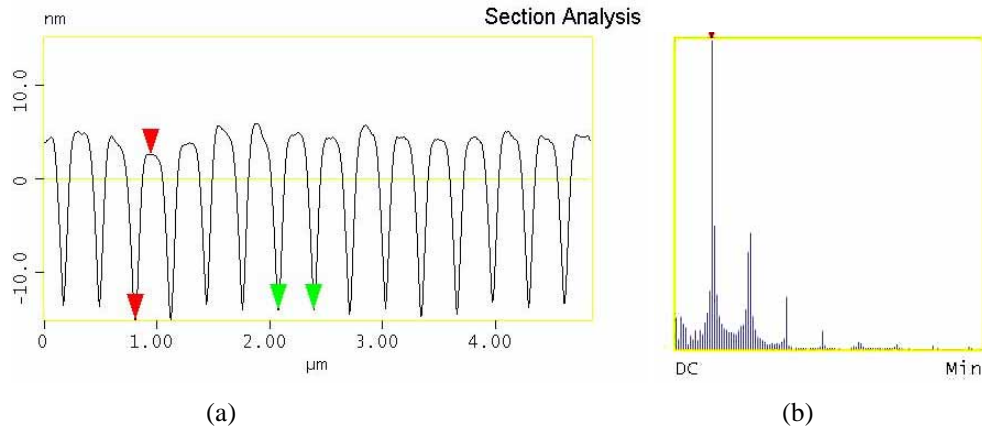


Fig. 3. (a) The profile of the grating 1 obtained with AFM. (b) The spatial spectrum obtained by Fourier transform of the profile.

In general, the results obtained by AFM characterization of various gratings, fabricated in this and the other experiments, indicate V-shape profile of the grooves of deep (more than 20 nm) corrugations and more irregular, close to sine, profiles of the shallow (less than 20 nm) gratings.

3. Optical characterization

To measure coupling efficiency the light beam from He-Ne laser (wavelength 632.8 nm, output power 2 mW) was focused on the grating coupler (see Fig. 4(a)). The diameter of the illumination spot was 5 mm before focusing. The elliptical beam spot on the gratings was formed by two cylindrical lenses: one with focal distance of 50 mm was used to squeeze the beam to 8 μm across the waveguide and the others, with focal lengths of 50, 75 and 200 mm, were used to elongate the beam along the waveguide providing spot lengths of approximately 8, 12, and 36 μm correspondingly. The spot dimensions were calculated using the data on the numerical apertures of the focusing optics. Light exiting the waveguides was collected at the output by an objective lens (magnification 60x, numerical aperture 0.85) and projected to a silicon photodetector (Hamamatsu S1337-33BR). The sample was placed on the rotation stage at an angle corresponding to the maximum coupling efficiency, the propagation constants of the corrugated waveguides modes were found (see Table1).

The coupling efficiency demonstrated strong dependence on the spot size (see Fig.4 (b)). The maximum efficiency for all the gratings was achieved with the lens of 50 mm focal length corresponding to approximately 8 μm beam waist in the focal point. The optimum coupling length is even less than this value and further excitation length shrinkage would lead to increase in the coupling efficiency. Starting from the value of 20 μm increase in the spot size results in slow decrease in coupling efficiency. This means that light entering the grating beside this distance does not reach the non corrugated part of the waveguide.

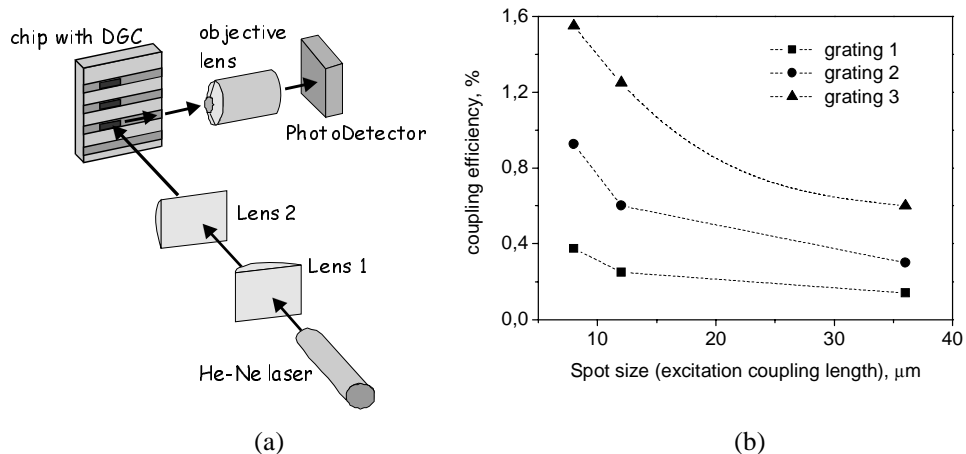


Fig. 4. (a) Schematic view of the experiment. (b) Measured coupling efficiencies of the DGCs versus incident beam spot size.

The length of light out-coupling from the waveguide on the DGC was estimated using the inverse scheme. Light was coupled into the waveguides with the gratings by direct focusing with an objective lens and the intensity distribution of light exiting the waveguide on the diffraction grating was observed using a microscope. The length of the out-coupling did not exceed $20 \mu\text{m}$.

4. Discussion

As it was mentioned above the radiation loss, which is usually square proportional to the corrugation depth, is inverse proportional to the optimum excitation length of the coupler. The example of that is presented in Fig. 5, where the optimized grating length needed for efficient coupling is plotted versus the corrugation depth.

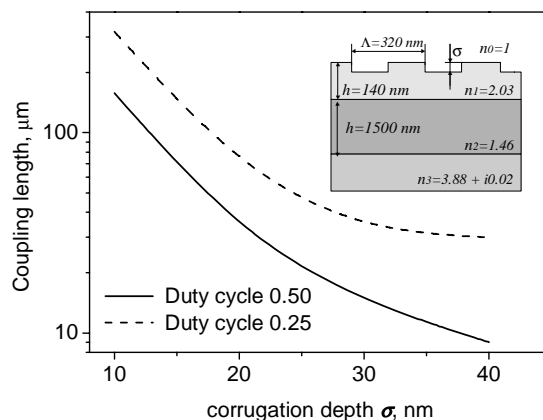


Fig. 5. Optimised coupling length versus corrugation depth for the grating couplers.

The simulations were done using the perturbation method following the procedure described elsewhere [13]. The curves are plotted for the waveguide with thickness of 140 nm and refractive index 2.03 deposited over silicon substrate and isolated of it by $1.5 \mu\text{m}$ thick silicon

dioxide layer with refractive index 1.46. The rectangular profile of the grating etched in the waveguide was assumed. The highest radiation loss (shortest coupling length) is observed for the corrugation profiles with duty cycle 0.5.

Power flow in and out of the corrugated waveguide with absorption losses and excited by an external light beam can be described by a differential equation [11]:

$$\frac{dP(x)}{dx} = A(x) \cdot \eta - P(x) \cdot \alpha_{rad} - P(x) \cdot \alpha_{abs} \quad (1)$$

Here $P(x)$ characterizes reduced field amplitude of the guided wave, $A(x)$ is the intensity distribution of the incident light, η defines the amount of light entering the waveguide, α_{rad} and α_{abs} are radiation and absorption losses on the grating. Both α_{rad} and α_{abs} influence the coupling length so that when the radiation losses are not high, the shrinkage of the length might take place due to absorption, i.e. $\alpha_{rad} \ll \alpha_{abs}$. In our experiments light entering the grating in the middle of it does not reach the non corrugated part of the waveguide because of high absorption inside the corrugated part, induced, apparently, by Ga implantation. In addition, implantation creates periodically modulated layer under the milled grating. This creates additional radiation losses, however, according to the simulations, they are smaller compared to absorption produced by this layer.

Auger spectrometry (PHI SAM-670) confirmed the presence of Ga in the gratings. Depth profiling was performed alternating AES analysis with ion sputtering on the grating 1. In Fig. 6 the normalized concentration of Ga is plotted as a function of depth. Ga was registered up to 100 nm deep in the grating.

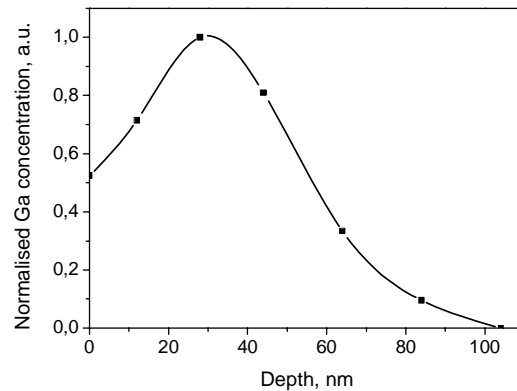


Fig. 6. Normalised depth profile of Ga inside the coupler.

To evaluate the refractive index of the modified silicon nitride a method of propagation modes was applied. The propagation constants found experimentally were different from the ones expected for the silicon nitride waveguides not modified by implantation (see Table 1). Implantation of metal particles of Ga into dielectric affects complex refractive index of the latter [14], mostly increasing the imaginary part, called extinction coefficient. The propagation constants of the modified waveguide were simulated using transfer matrix approach. The waveguide was represented as a three layer structure. The first layer, 20 nm thick, was the milled grating. The second one was a layer of silicon nitride periodically modified under the grating grooves by implanted gallium. This layer was assumed to have thickness of 70 nm. The third layer, 50 nm thick, was silicon nitride not affected by implantation. The refractive index of the second layer was adjusted to fit the propagation constants with the experimentally obtained values. The absolute value of the effective

refractive index of the implanted area was found to be 2.2. In reality, the index is gradually changing across the waveguide matching the distribution of implanted gallium inside the film. Local changes of the index in the area where the gallium concentration reaches its maximum might be higher.

Experiments on optimization of the ion beam parameters are the subject of our current work. The energy of the ions could be adjusted so that they would not penetrate deep into the waveguides, but just produce sputtering of the target material [8].

5. Summary

The diffraction grating couplers were fabricated on Si_3N_4 waveguides using focused ion beam milling. They were tested using excitation with visible light. The couplers work, although the coupling efficiency was lower than expected, which was a consequence of Ga implantation into the waveguides. Implantation of gallium can be considered as modification of silicon nitride refractive index, which became a complex value with an increased extinction coefficient. Implanted Ga introduced high absorption losses which are dominating the diffraction produced by surface corrugation. Absorption significantly shortened the excitation coupling length and decreased the coupling efficiency of the devices.

Acknowledgements

Authors acknowledge European Union (IST-2001-37239) for the financial support.